

Supporting Information

A tetrานuclear Pr-W heterometal cluster-imbedded antimotungstate for catalytic synthesis of benzimidazoles

Zhijian Zheng,^{†a} Song Jiang,^{†a} Xuejiao Chen,^{†a} Haoqi Liu,^a Yufeng Liu,^a Yayu Dong,^b Xiaopeng Sun
^{*c} and Guoping Yang ^{*a}

^aSchool of Chemistry and Materials Science, Jiangxi Key Laboratory for Mass Spectrometry and Instrumentation, East China University of Technology, Nanchang, Jiangxi 330013, P. R. China.

^bSchool of Materials Science and Engineering, East China Jiaotong University, Nanchang, Jiangxi, 330013, China.

^cHenan Key Laboratory of Polyoxometalate Chemistry, Institute of Molecular and Crystal Engineering, School of Chemistry and Chemical Engineering, Henan University, Kaifeng, Henan, 475004, China.

[†]These authors contributed equally to this work.

Email: xpsun@henu.edu.cn; erick@ecut.edu.cn.

Table of Contents

1. General Information	2
2. Experimental.....	2
3. Characterization.....	4
4. Characterization of Products	9
5. Notes and References	24

1. General Information

Materials and Methods

All reagents were obtained from commercial sources and used without further purification.

The FT-IR spectrum was obtained by using a Fourier transform infrared (FT-IR) (4000-500 cm⁻¹) spectrometer (Thermo Nicolet iS5) at 0.5 cm⁻¹ resolution and 16 scans. Thermogravimetric analyses (TGA) were performed under an N₂ atmosphere on Mettler-Toledo TGA/SDTA 851^e thermal analyzer from 30 to 800 °C. Powder X-ray diffraction (PXRD) was performed on a Bruker D8 Advance diffractometer with Cu K α radiation ($\lambda = 1.5406 \text{ \AA}$) at room temperature. Inductively coupled plasma optical emission spectrum (ICP-OES) data were obtained on an Agilent 725 ICP-OES spectrometer. Elemental analyses (EA) (C, H, and N) were performed on a Vario EL Cube CHN elemental analyzer. The solid-state ultraviolet diffuse reflection spectrum was acquired on a UV-8000 ultraviolet and visible spectrophotometer equipping an integrating sphere (Shanghai Metash Instruments Co., Ltd). Flash column chromatography was performed using silica gel of 200-300 mesh. The GC analysis was performed on Agilent 7890B equipped with a capillary column (HP-5, 30 m × 0.25 μm) using a flame ionization detector. The GC-MS were recorded on Agilent 7890B-7000D.

X-ray Crystallography

The single crystal X-ray diffraction data were collected on Bruker D8 VENTURE diffractometer with graphite monochromated Mo K α radiation ($\lambda = 0.71073 \text{ \AA}$). Intensities were collected by ω -scan and reduced on *APEX 3* and a multi-scan absorption correction was applied.¹ The structures were solved and refined on *Olex2* using the *SHELX* package.² Parameters of the crystal data collection and refinement are given in Table S1. The CCDC number is 2373492.

2. Experimental

Synthesis of Pr-1

Na₂WO₄·2H₂O (6 mmol, 1.9791 g), SbCl₃ (0.8 mmol, 0.1825 g), (CH₃)₂NH₂Cl (12 mmol, 0.9785 g), and DL-tartaric acid (0.3 mmol, 0.0451 g) were sequentially dissolved in a 0.5 M pH = 4.8 NaAc/HAc solution. The solution was adjusted to pH = 4.5 using 6 M HCl and stirred for 10 min. PrCl₃·6H₂O (0.6 mmol, 0.2132 g) was subsequently added to the solution and the pH was adjusted to 4.0 after the solids were completely dissolved. The clear green solution was stirred for another 10 min before being filtered. The green filtrate was left to evaporate at room temperature. Colorless stick crystals were collected after about six weeks (yield: 35% based on PrCl₃·6H₂O).

Elemental analysis for $C_{22}H_{140.6}N_4Cl_{0.5}Na_{20.5}O_{214.3}Pr_4Sb_4W_{42}$ ($Mr = 13151.555$) (%): found (calc.): C, 2.05 (2.01); H, 1.01 (1.08), N, 0.39 (0.43); Na, 3.62 (3.58); Pr, 4.28 (4.29); W, 58.72 (58.71).

FT-IR (cm^{-1}): 3388 (m), 3155 (m), 2794 (w), 1611 (m), 1538 (m), 1464 (m), 1407 (m), 1370 (m), 1169 (w), 1136 (w), 1071 (w), 1017 (w), 936 (s), 833 (vs), 763 (vs), 680 (vs), 598 (vs).

Formula: $[(\text{CH}_3)_2\text{NH}_2]_4\text{Na}_{20.5}\{[(\text{OAc})\text{Pr}_4\text{W}_6\text{O}_{12}(\text{tar})_3](\text{SbW}_9\text{O}_{33})_4(\text{H}_2\text{O})_{10}\}\text{Cl}_{0.5}\text{ca.}40.3\text{H}_2\text{O}$.

Typical procedure of the three-component reaction

To a 4 mL reaction vial, benzaldehyde (**1a**, 0.2 mmol) and *o*-phenylenediamine (**2a**, 0.2 mmol), **Pr-1** (0.2 mol%), and EtOH (1 mL) were added. Then the reaction was carried out in screw cap vials with a Teflon seal at 100 °C for 1 h under an oxygen atmosphere. After the reaction, the mixture was purified by column chromatography (petroleum ether/EtOAc) or recrystallization to afford the desired products.

3. Characterization

Table S1. Crystallographic data and structure refinement of **Pr-1** (SQUEEZE).

CCDC	2373492
Empirical formula	C ₁₄ H ₉ Cl _{0.5} Na ₅ O ₁₇₇ Pr ₄ Sb ₄ W ₄₂
Formula weight	11914.23
Temperature (K)	100
Crystal system	triclinic
Space group	<i>P</i> -1
<i>a</i> (Å)	13.5636(8)
<i>b</i> (Å)	19.4915(11)
<i>c</i> (Å)	48.477(3)
α (°)	85.183(2)
β (°)	85.802(2)
γ (°)	69.864(2)
<i>V</i> (Å ³)	11976.9(12)
<i>F</i> (000)	10241.0
<i>Z</i>	2
ρ_{calcd} (g·cm ⁻³)	3.304
μ (mm ⁻¹)	21.410
Crystal size (mm ³)	0.52 × 0.38 × 0.33
2θ range for data collection (°)	4.45 to 50
Index ranges	-16 ≤ <i>h</i> ≤ 16, -23 ≤ <i>k</i> ≤ 23, -57 ≤ <i>l</i> ≤ 57
Reflections collected	123886
Independent reflections	41574 [$R_{\text{int}} = 0.0830$, $R_{\text{sigma}} = 0.0899$]
Restraints	3358
Parameter	2252
GOOF on F^2	1.092
R_1^{a} [$I \geq 2\sigma(I)$]	0.1018
wR_2^{b} (all data)	0.2823
Largest diff. peak/hole (e Å ⁻³)	6.06/-3.65

$$^{\text{a}}R_1 = \sum ||F_o| - |F_c|| / \sum |F_o|, ^{\text{b}}wR_2 = \{\sum [w(F_o^2 - F_c^2)^2] / \sum [w(F_o^2)^2]\}^{1/2}$$

Table S2. Bond valence calculations for Pr, Sb, and W atoms in **Pr-1**.

Atom	BVS	Valence	Atom	BVS	Valence
Pr1	3.33	+3	Sb1	2.96	+3
Pr22	3.26	+3	Sb2	2.85	+3
Pr33	3.26	+3	Sb3	2.91	+3
Pr4	3.33	+3	Sb4	2.90	+3
W1	6.04	+6	W22	5.77	+6
W2	5.80	+6	W23	5.94	+6
W3	6.28	+6	W24	5.86	+6
W4	5.79	+6	W25	6.13	+6
W5	5.74	+6	W26	5.79	+6
W6	6.07	+6	W27	6.03	+6
W7	5.89	+6	W28	5.89	+6
W8	6.07	+6	W29	5.89	+6
W9	5.96	+6	W30	6.09	+6
W10	6.19	+6	W31	5.77	+6
W11	5.98	+6	W32	6.09	+6
W12	6.14	+6	W33	6.21	+6
W13	6.11	+6	W34	5.91	+6
W14	5.81	+6	W35	6.16	+6
W15	6.16	+6	W36	5.72	+6
W16	5.92	+6	W37	6.01	+6
W17	5.95	+6	W38	5.70	+6
W18	6.04	+6	W39	6.07	+6
W19	5.96	+6	W40	6.24	+6
W20	6.04	+6	W41	5.78	+6
W21	6.06	+6	W42	6.03	+6

Bond valence sum (BVS) analysis: The BVS values (V_i) of metal atoms were calculated using the following equation:³

$$V_i = \sum \exp[(r_0 - r_{ij})/B] \quad (1)$$

where r_0 is the bond valence parameter for a given atom pair, r_{ij} is the bond length between atoms i and j obtained from the crystal structure.

Table S3 Selected bond lengths [Å] and angles [°] for **Pr-1**.

W1-O3	1.735(16)	W32-O76	1.878(16)
W1-O4	1.799(17)	W32-O101	1.768(19)
W1-O5	1.892(19)	W32-O102	1.788(16)
W1-O6	2.149(16)	W32-O103	1.950(15)
W1-O10L	1.960(19)	W32-O104	2.129(19)
W1-O11L	2.155(16)	W33-O103	1.903(16)
W2-O5	2.013(17)	W33-O109	1.723(16)
W2-O11	1.732(18)	W33-O115	1.959(19)
W2-O17	1.938(19)	W33-O116	1.856(19)
W2-O18	1.916(18)	W33-O122	1.878(17)
W2-O24	1.886(18)	W33-O144	2.275(17)
W2-O136	2.323(17)	W34-O104	1.794(18)
W3-O6	1.769(16)	W34-O110	1.709(14)
W3-O12	1.733(19)	W34-O116	1.994(18)
W3-O18	1.907(19)	W34-O117	1.944(18)
W3-O19	1.912(17)	W34-O123	2.048(17)
W3-O25	2.023(17)	W34-O145	2.356(18)
W3-O135	2.312(18)	W35-O105	1.756(19)
W4-O7	1.800(17)	W35-O111	1.738(18)
W4-O13	1.764(19)	W35-O117	1.950(18)
W4-O19	1.968(17)	W35-O118	1.924(17)
W4-O20	1.913(18)	W35-O124	2.071(18)
W4-O26	2.094(17)	W35-O145	2.223(18)
W4-O135	2.239(19)	W36-O106	1.799(17)
W5-O8	1.805(17)	W36-O112	1.762(19)
W5-O14	1.747(17)	W36-O118	1.930(19)
W5-O20	1.937(18)	W36-O119	2.01(2)
W5-O21	1.992(19)	W36-O125	2.080(18)
W5-O27	2.097(17)	W36-O146	2.229(18)
W5-O137	2.244(18)	W37-O107	1.842(17)
W6-O9	1.808(16)	W37-O113	1.718(19)
W6-O15	1.72(2)	W37-O119	1.908(18)
W6-O21	1.911(19)	W37-O120	1.987(17)
W6-O22	1.955(17)	W37-O126	1.970(18)
W6-O28	2.027(16)	W37-O146	2.31(2)
W6-O137	2.310(18)	W38-O108	1.965(16)
W7-O10	1.926(17)	W38-O114	1.76(2)
W7-O16	1.765(19)	W38-O115	1.980(17)
W7-O17	1.948(18)	W38-O120	1.861(17)
W7-O22	1.899(16)	W38-O121	1.914(18)
W7-O23	1.900(17)	W38-O144	2.265(19)
W7-O136	2.261(19)	W39-O121	1.96(2)

W8-O23	2.046(18)	W39-O122	2.024(17)
W8-O24	1.977(18)	W39-O127	1.857(17)
W8-O29	1.873(17)	W39-O128	1.829(19)
W8-O30	1.808(19)	W39-O131	1.738(17)
W8-O33	1.737(18)	W39-O144	2.221(17)
W8-O136	2.241(17)	W39-W33A	2.97(6)
W9-O25	1.936(18)	W40-O123	1.868(18)
W9-O26	1.82(2)	W40-O124	1.868(18)
W9-O30	2.036(19)	W40-O128	2.017(18)
W9-O31	1.903(18)	W40-O129	1.901(18)
W9-O34	1.752(15)	W40-O132	1.69(2)
W9-O135	2.278(16)	W40-O145	2.350(18)
W10-O27	1.871(18)	W41-O125	1.880(19)
W10-O28	1.852(18)	W41-O126	1.97(2)
W10-O29	1.972(18)	W41-O127	2.013(18)
W10-O31	1.928(19)	W41-O129	1.925(19)
W10-O32	1.713(17)	W41-O130	1.721(13)
W10-O137	2.359(17)	W41-O146	2.299(17)
W11-O9	2.108(16)	W42-Na1	3.580(11)
W11-O10	1.919(16)	W42-Na2	3.584(15)
W11-O35	1.766(18)	W42-O16L	1.991(18)
W11-O36	1.800(16)	W42-O17L	2.184(17)
W11-O37	1.928(15)	W42-O107	2.078(17)
W11-O38	2.134(18)	W42-O108	1.901(17)
W12-O37	1.921(16)	W42-O133	1.762(18)
W12-O43	1.722(16)	W42-O134	1.764(17)
W12-O49	1.962(18)	Pr1-Na3	4.126(14)
W12-O50	1.886(18)	Pr1-O1	2.357(19)
W12-O56	1.885(15)	Pr1-O1L	2.57(2)
W12-O140	2.267(16)	Pr1-O1W	2.590(18)
W13-O38	1.790(17)	Pr1-O2L	2.586(18)
W13-O44	1.728(19)	Pr1-O3	2.581(16)
W13-O50	1.972(17)	Pr1-O7	2.453(16)
W13-O51	1.924(16)	Pr1-O8	2.499(18)
W13-O57	1.990(17)	Pr1-O35	2.436(18)
W13-O138	2.285(18)	Pr1-O68	2.545(17)
W14-O39	1.769(17)	Pr1-C1	2.93(3)
W14-O45	1.760(17)	Pr2-Sb2	3.717(2)
W14-O51	1.984(18)	Pr2-O2W	2.54(2)
W14-O52	1.959(17)	Pr2-O3W	2.454(19)
W14-O58	2.089(16)	Pr2-O4	2.455(17)
W14-O138	2.228(16)	Pr2-O4W	2.589(18)
W15-O40	1.769(17)	Pr2-O36	2.323(16)
W15-O46	1.736(18)	Pr2-O39	2.485(18)

W15-O52	1.886(19)	Pr2-O40	2.480(17)
W15-O53	1.984(18)	Pr2-O67	2.494(17)
W15-O59	2.038(17)	Pr3-Na1	4.152(10)
W15-O139	2.250(16)	Pr3-Na2	4.153(13)
W16-O41	1.798(16)	Pr3-O2	2.373(19)
W16-O47	1.754(17)	Pr3-O5W	2.553(18)
W16-O53	1.923(16)	Pr3-O7L	2.70(2)
W16-O54	1.995(16)	Pr3-O8L	2.55(2)
W16-O60	1.984(17)	Pr3-O69	2.567(18)
W16-O139	2.297(18)	Pr3-O73	2.456(17)
W17-O42	2.002(17)	Pr3-O74	2.534(19)
W17-O48	1.740(19)	Pr3-O101	2.432(19)
W17-O49	1.953(16)	Pr3-O134	2.561(17)
W17-O54	1.850(16)	Pr3-C5	2.97(3)
W17-O55	1.889(16)	Pr4-O6W	2.58(2)
W17-O140	2.308(18)	Pr4-O7W	2.49(2)
W18-O55	2.014(17)	Pr4-O8W	2.528(18)
W18-O56	2.009(16)	Pr4-O70	2.425(18)
W18-O61	1.885(17)	Pr4-O102	2.316(17)
W18-O62	1.816(19)	Pr4O105	2.503(19)
W18-O65	1.726(17)	Pr4-O106	2.451(17)
W18-O140	2.240(16)	Pr4-O133	2.470(19)
W19-O57	1.858(17)	Sb1-O135	1.998(17)
W19-O58	1.868(16)	Sb1-O136	1.971(19)
W19-O62	2.023(17)	Sb1-O137	2.021(17)
W19-O63	1.985(18)	Sb2-O138	2.010(18)
W19-O66	1.705(18)	Sb2-O139	1.989(16)
W19-O138	2.385(17)	Sb2-O140	1.979(16)
W20-O59	1.877(17)	Sb3-O141	2.010(17)
W20-O60	1.929(18)	Sb3-O142	1.981(18)
W20-O61	1.971(17)	Sb3-O143	2.017(18)
W20-O63	1.854(19)	Sb4-O144	1.998(16)
W20-O64	1.752(16)	Sb4-O145	2.004(19)
W20-O139	2.308(16)	Sb4-O146	2.002(17)
W21-Na1	3.582(11)	Na1-Na3	3.712(18)
W21-Na3	3.692(17)	Na1-O1	2.53(2)
W21-O13L	2.238(17)	Na1-O2	2.488(19)
W21-O15L	1.921(18)	Na1-O9W	2.340(19)
W21-O41	2.116(16)	Na1-O10W	2.42(2)
W21-O42	1.896(18)	Na1-O15L	2.65(2)
W21-O67	1.755(17)	Na1-O16L	2.634(19)
W21-O68	1.778(17)	Na1-O68	2.82(2)
W22-O4L	2.005(19)	Na1-O134	2.81(2)
W22-O5L	2.155(17)	Na1-C13	2.84(3)

W22-O69	1.739(18)	Na2-O7L	2.31(2)
W22-O70	1.824(18)	Na2-O9W	2.40(2)
W22-O71	1.918(18)	Na2-C11	2.718(19)
W22-O72	2.130(17)	Na2-O17L	2.45(2)
W23-O71	1.951(17)	Na2-O134	2.69(2)
W23-O78	1.765(17)	Na2-O12W	2.08(4)
W23-O84	1.948(18)	Na3-O1L	2.22(2)
W23-O85	1.874(18)	Na3-O10W	2.36(2)
W23-O91	1.884(18)	Na3-O15W	2.45(5)
W23-O142	2.270(17)	Na3-O13L	2.61(2)
W24-O72	1.815(17)	Na3-O13W	2.37(2)
W24-O79	1.74(2)	Na3-O68	2.74(2)
W24-O85	1.980(19)	Na3-O15X	2.38(6)
W24-O86	1.949(19)	Na4-O5L	2.84(2)
W24-O92	1.986(17)	Na4-O6L	2.55(2)
W24-O141	2.308(18)	Na4-O78	2.53(2)
W25-O73	1.780(18)	Na4-O811	2.44(2)
W25-O80	1.714(19)	Na4-C4	3.10(3)
W25-O86	1.943(18)	Na4-O14W	2.33(3)
W25-O87	1.926(19)	Na5-O11	2.45(2)
W25-O93	2.101(17)	Na5-O11L	2.73(2)
W25-O141	2.225(19)	Na5-O12L	2.56(2)
W26-O74	1.783(18)	Na5-O142	2.43(2)
W26-O81	1.747(18)	Na5-C8	2.94(3)
W26-O87	1.935(19)	O1-C13	1.24(3)
W26-O88	1.984(19)	O1L-C1	1.24(3)
W26-O94	2.103(19)	O2-C13	1.32(3)
W26-O143	2.257(18)	O2L-C1	1.27(3)
W27-O75	1.786(17)	O3L-C2	1.49(3)
W27-O82	1.714(19)	O4L-C3	1.39(3)
W27-O83	1.971(17)	O5L-C4	1.28(4)
W27-O88	1.923(18)	O6L-C4	1.30(3)
W27-O89	2.072(17)	O7L-C5	1.18(3)
W27-O143	2.290(18)	O8L-C5	1.26(3)
W28-O76	1.984(17)	O9L-C6	1.45(3)
W28-O77	1.740(19)	O10L-C7	1.43(3)
W28-O83	1.885(17)	O11L-C8	1.30(3)
W28-O84	1.981(17)	O12L-C8	1.21(3)
W28-O90	1.885(18)	O13L-C9	1.30(3)
W28-O142	2.251(18)	O14L-C9	1.27(3)
W29-O90	2.032(18)	O15L-C10	1.48(3)
W29-O91	2.025(18)	O16L-C11	1.33(3)
W29-O95	1.844(17)	O17L-C12	1.38(3)
W29-O96	1.847(19)	O18L-C12	1.18(3)

W29-O99	1.747(19)	O109-W33A	1.90(6)
W29-O142	2.260(17)	O116-W33A	1.56(6)
W30-O92	1.897(18)	O122-W33A	1.32(6)
W30-O93	1.828(19)	O144-W33A	2.46(6)
W30-O96	2.025(18)	C1-C2	1.49(4)
W30-O97	1.903(18)	C2-C3	1.57(4)
W30-O100	1.737(17)	C3-C4	1.43(4)
W30-O141	2.274(17)	C5-C6	1.52(4)
W31-O89	1.883(18)	C6-C7	1.57(4)
W31-O94	1.86(2)	C7-C8	1.564(18)
W31-O95	2.037(18)	C9-C10	1.51(4)
W31-O97	1.926(19)	C10-C11	1.559(19)
W31-O98	1.769(18)	C11-C12	1.57(3)
W31-O143	2.356(18)	C13-C14	1.52(4)
W32-O75	2.111(17)		

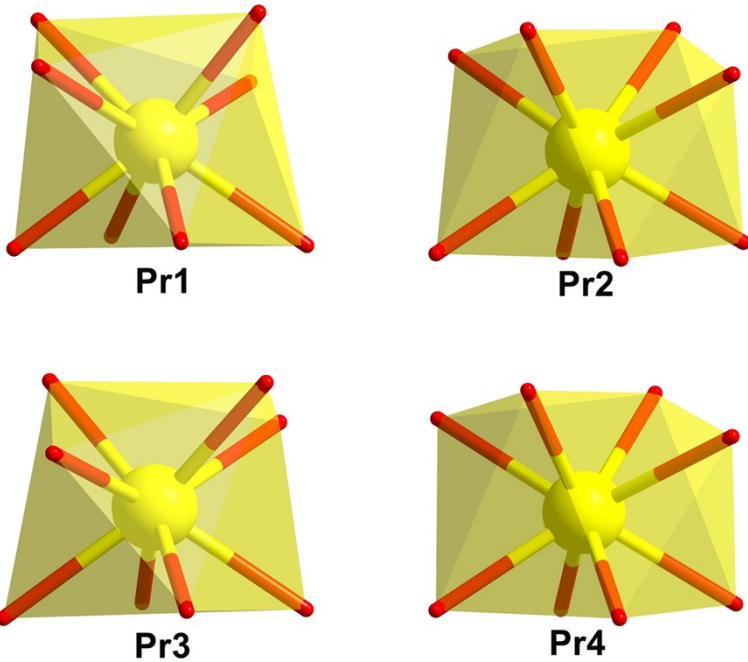


Figure S1. The coordination environment of Pr1-Pr4.

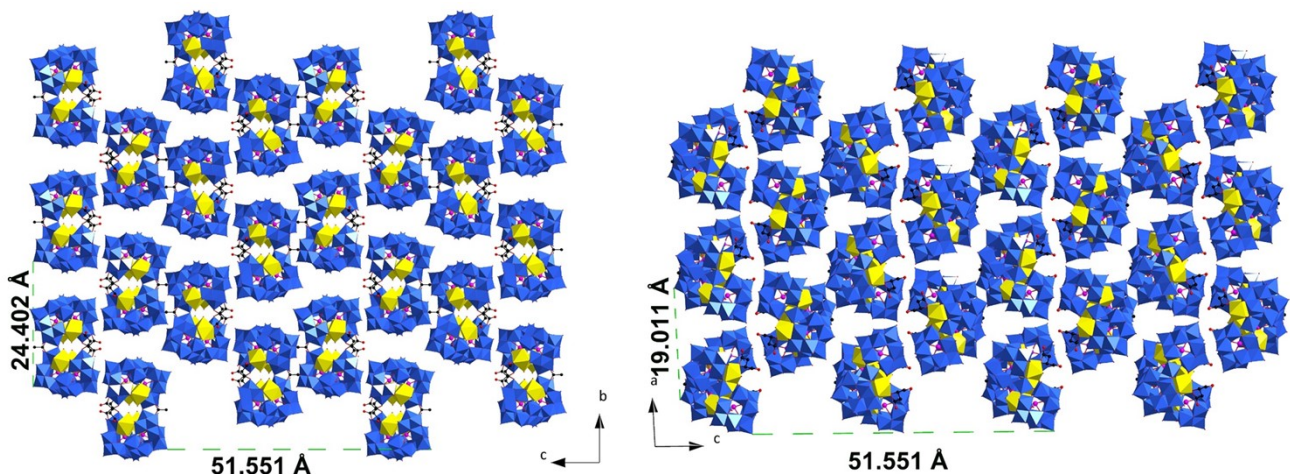


Figure S2. The packing view of **Pr-1** along the *a*-axis, and *b*-axis.

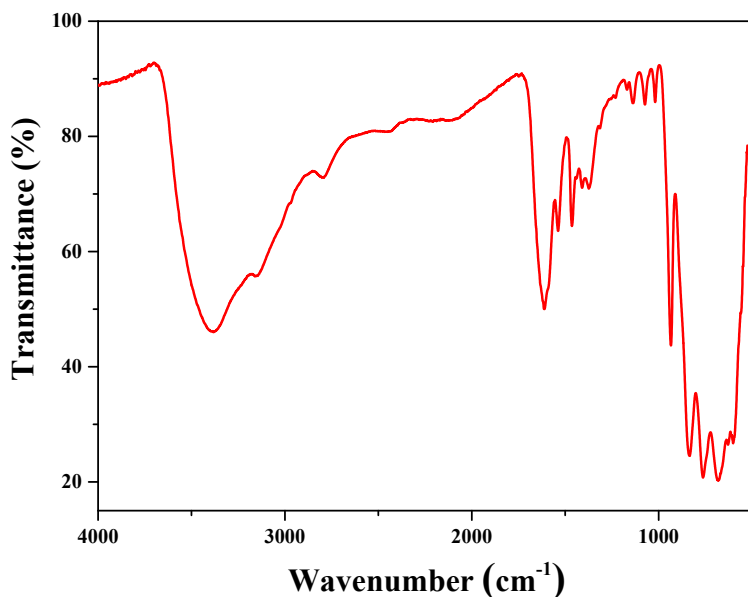


Figure S3. FT-IR spectra of Pr-1.

The broad absorption peaks at about 3388 cm^{-1} and 1611 cm^{-1} are attributed to the $\nu(\text{O}-\text{H})$ stretching vibration of water. The $\nu(\text{N}-\text{H})$ and $\nu(\text{C}-\text{H})$, and $\nu(\text{C}-\text{N})$ from the stretching vibrations of $(\text{CH}_3)_2\text{NH}_2$ cations are at 3155, 2794, 1464 and 1017 cm^{-1} . Other peaks (1538 , 1407 , 1370 , 1169 , 1136 , and 1071 cm^{-1}) are assigned to be the vibrations of C-H, C-C and C-O bonds in tar ligands. The peaks that appear in the range of 500 to 1000 cm^{-1} are be attributed to the stretching vibrations of $\nu(\text{W}-\text{O}_t)$, $\nu(\text{Sb}-\text{O})$, $\nu(\text{W}-\text{O}_b)$, and $\nu(\text{W}-\text{O}_c)$, and the absorption peaks appearing at 936 , 833 , 763 , 680 , and 598 cm^{-1} , respectively.

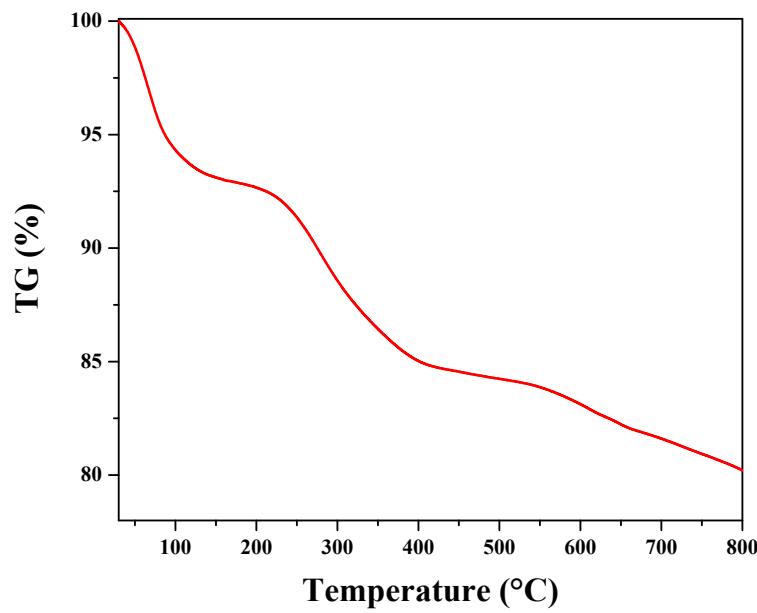
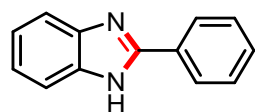


Figure S4. TGA curve of Pr-1.

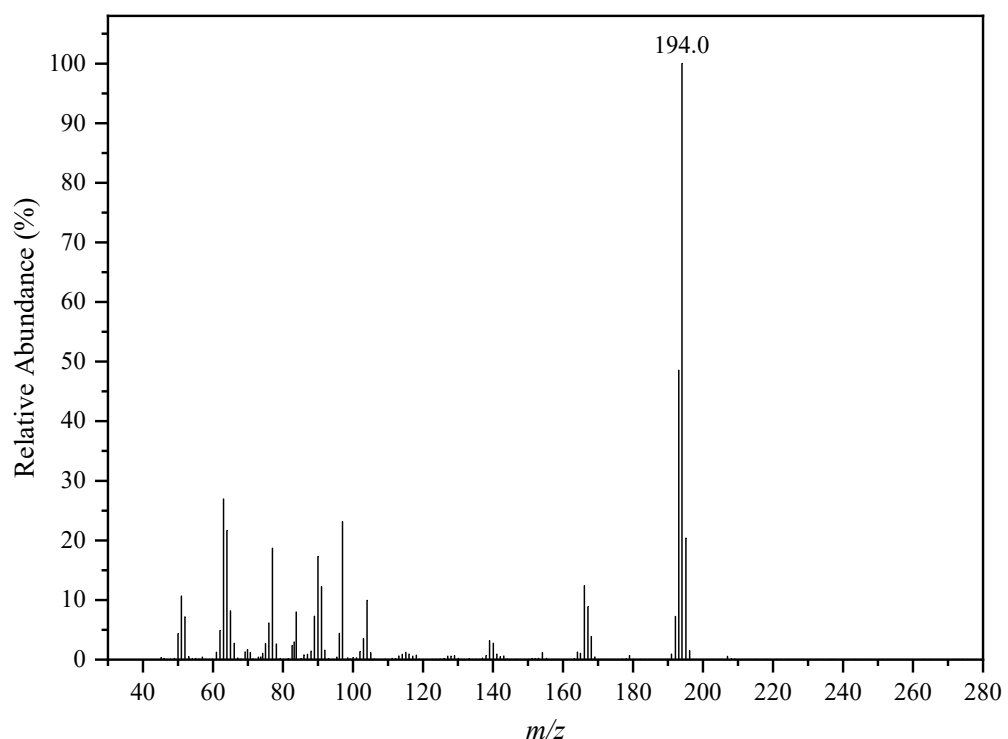
Thermalgravimetric analysis was performed on the crystalline samples under N₂ atmosphere from 30 to 800 °C. The weight loss at 150 °C is about 6.89%, which corresponds to the loss of ~50.3 water molecules.

4. Characterization of Products

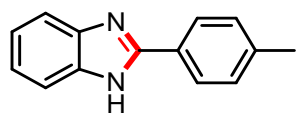
2-phenyl-1*H*-benzo[*d*]imidazole (3a)



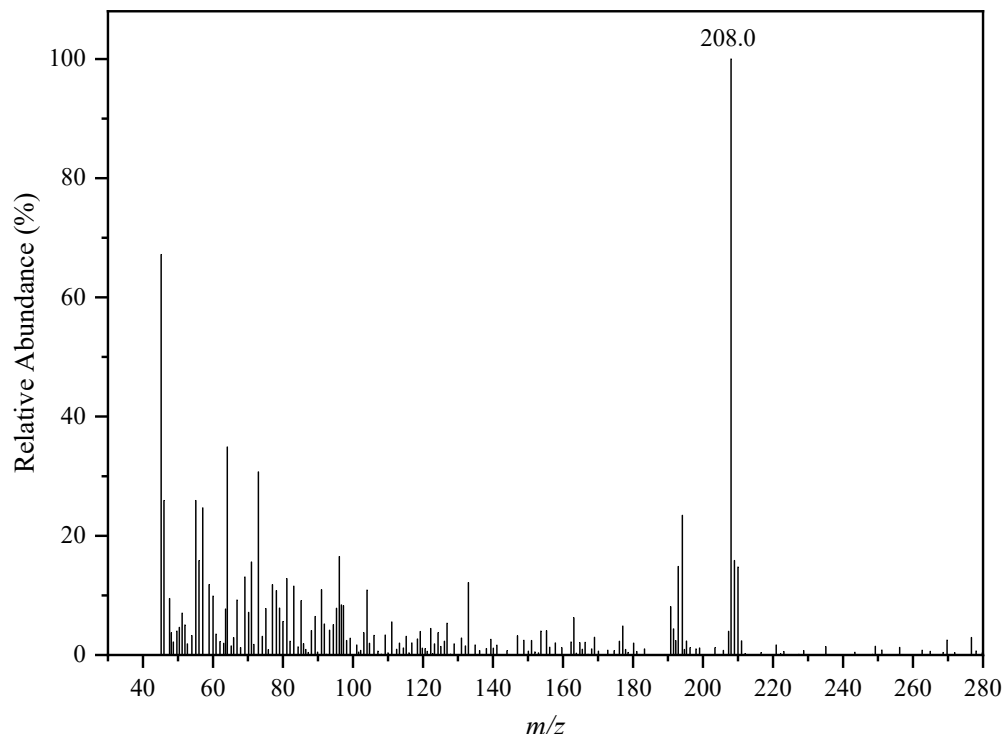
EI-MS: C₁₃H₁₀N₂, m/z (%) = 194.0 (100%) [M⁺].



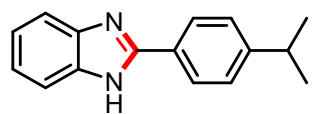
2-(*p*-tolyl)-1*H*-benzo[*d*]imidazole (3b)



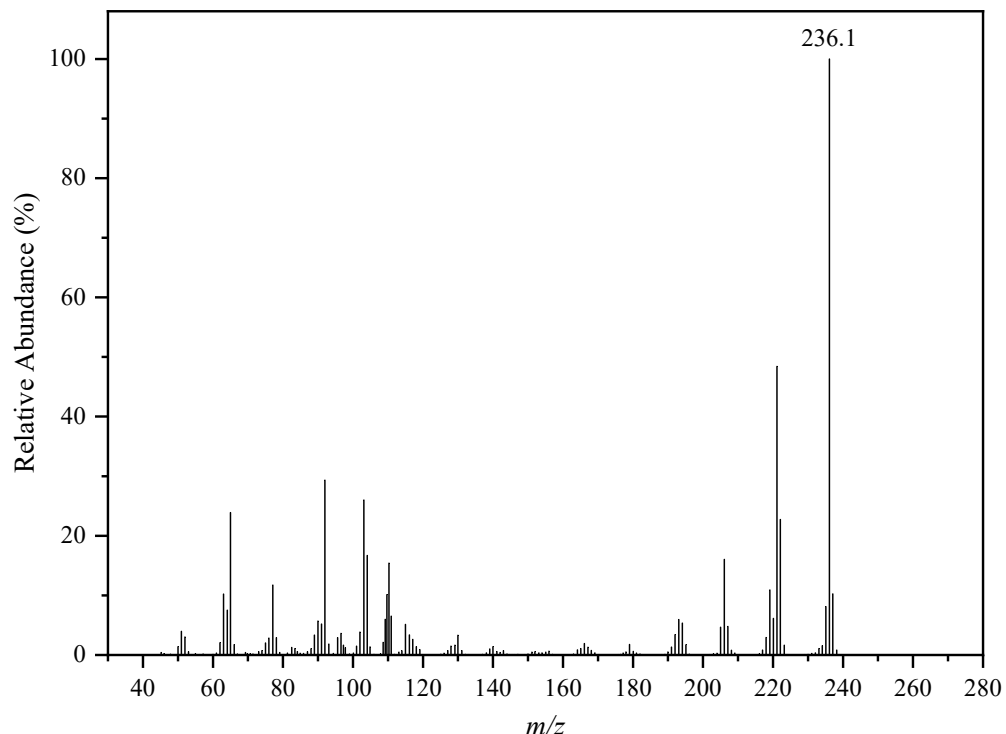
EI-MS: C₁₄H₁₂N₂, m/z (%) = 208.0 (100%) [M⁺].



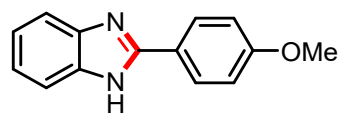
2-(4-isopropylphenyl)-1*H*-benzo[*d*]imidazole (3c)



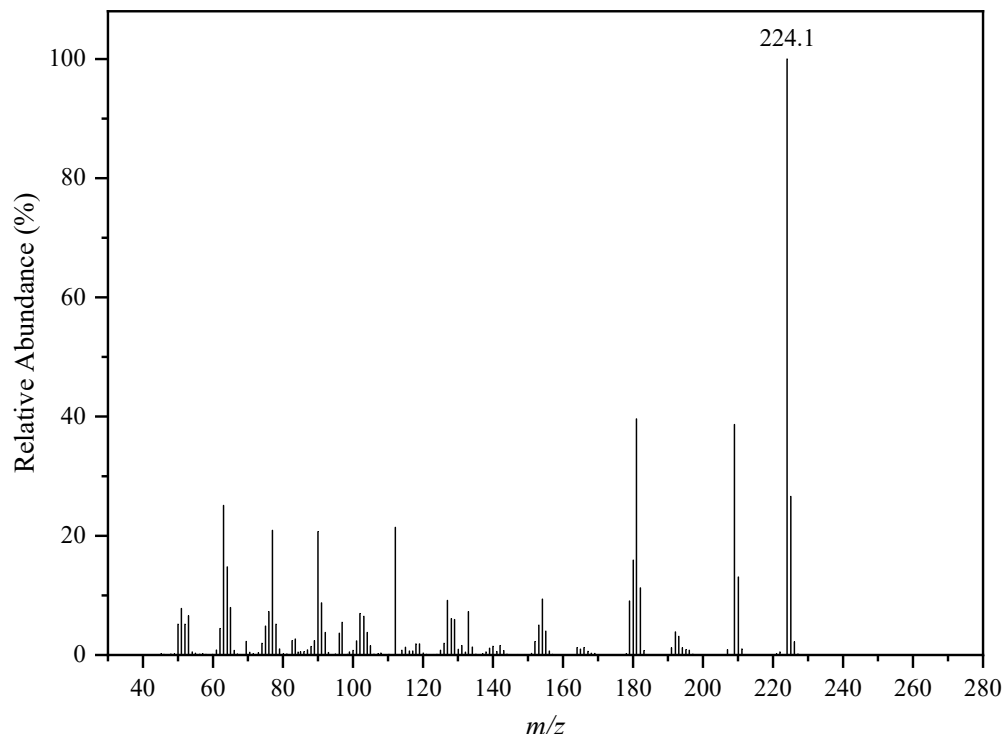
EI-MS: C₁₆H₁₆N₂, m/z (%) = 236.1 (100%) [M⁺].



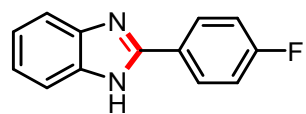
5-methoxy-2-phenyl-1*H*-benzo[*d*]imidazole (3d)



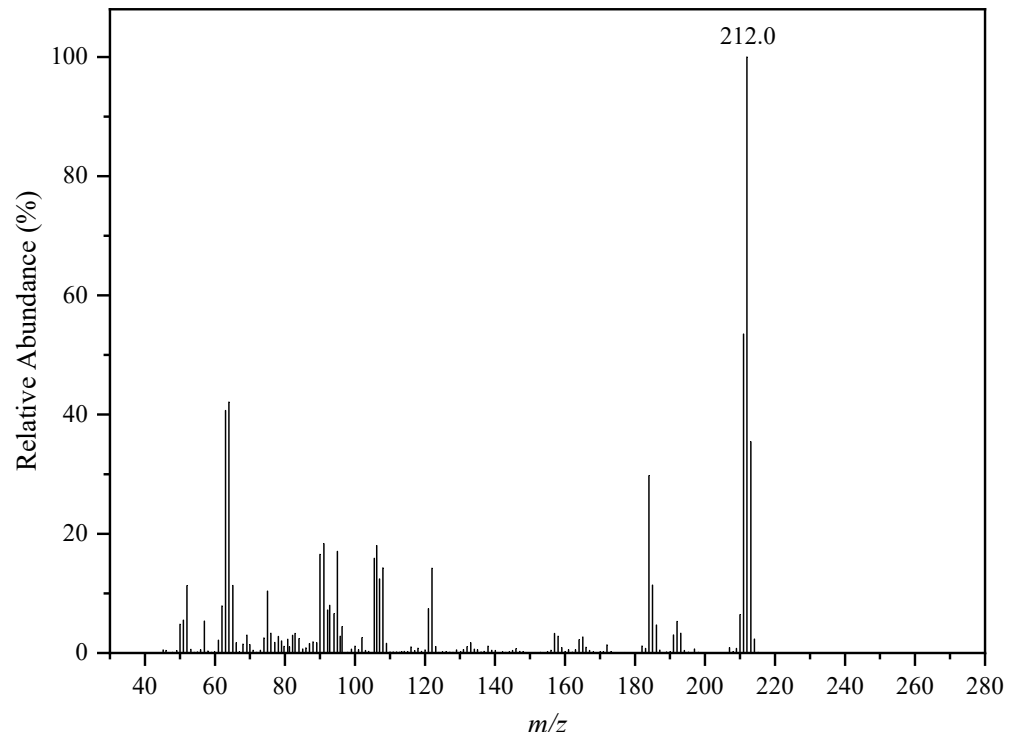
EI-MS: C₁₄H₁₂N₂O, m/z (%) = 224.1 (100%) [M⁺].



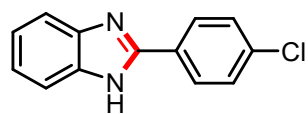
2-(4-fluorophenyl)-1*H*-benzo[*d*]imidazole (3e)



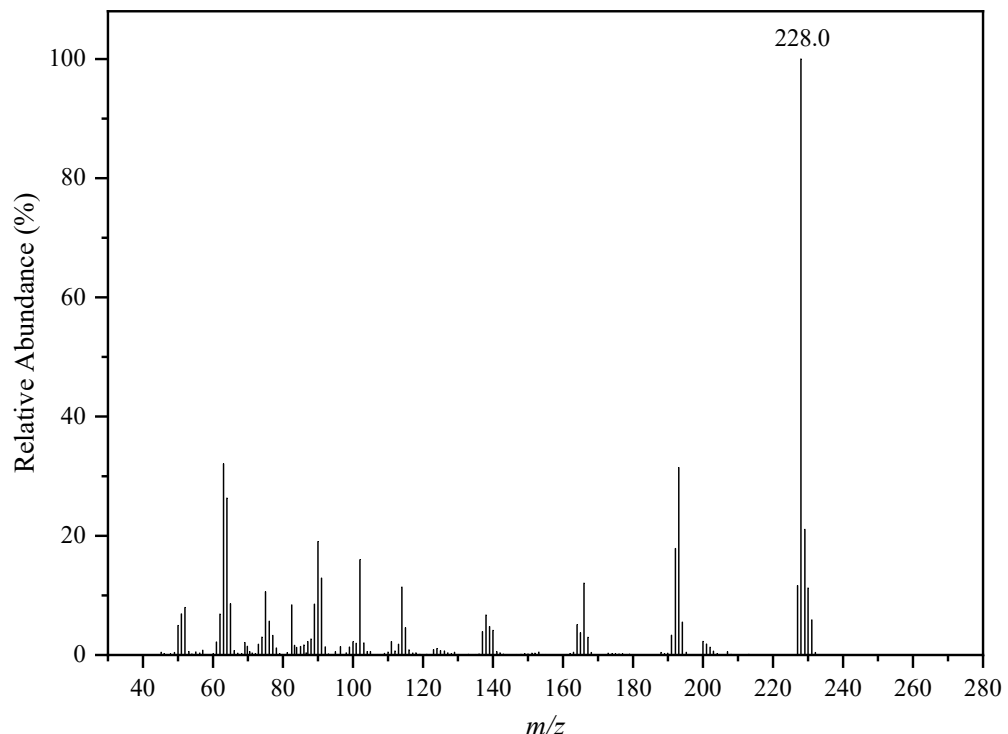
EI-MS: C₁₃H₉FN₂, m/z (%) = 212.0 (100%) [M⁺].



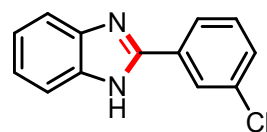
2-(4-chlorophenyl)-1*H*-benzo[*d*]imidazole (3f)



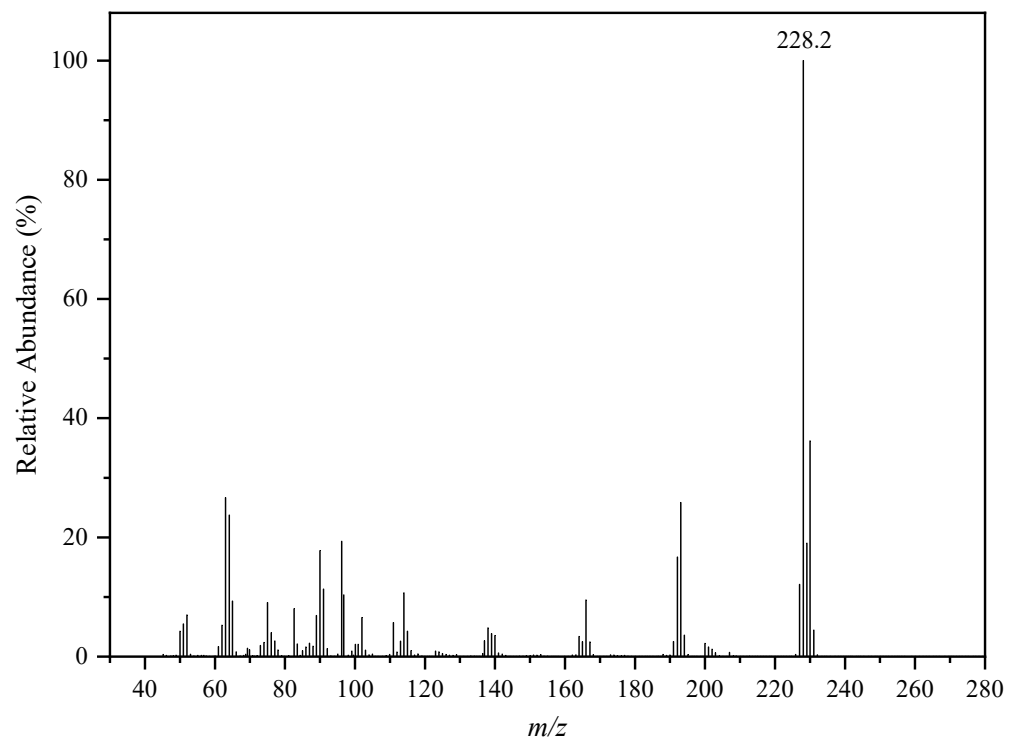
EI-MS: C₁₃H₉ClN₂, m/z (%) = 228.0 (100%) [M⁺].



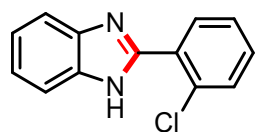
2-(3-chlorophenyl)-1*H*-benzo[*d*]imidazole (3g)



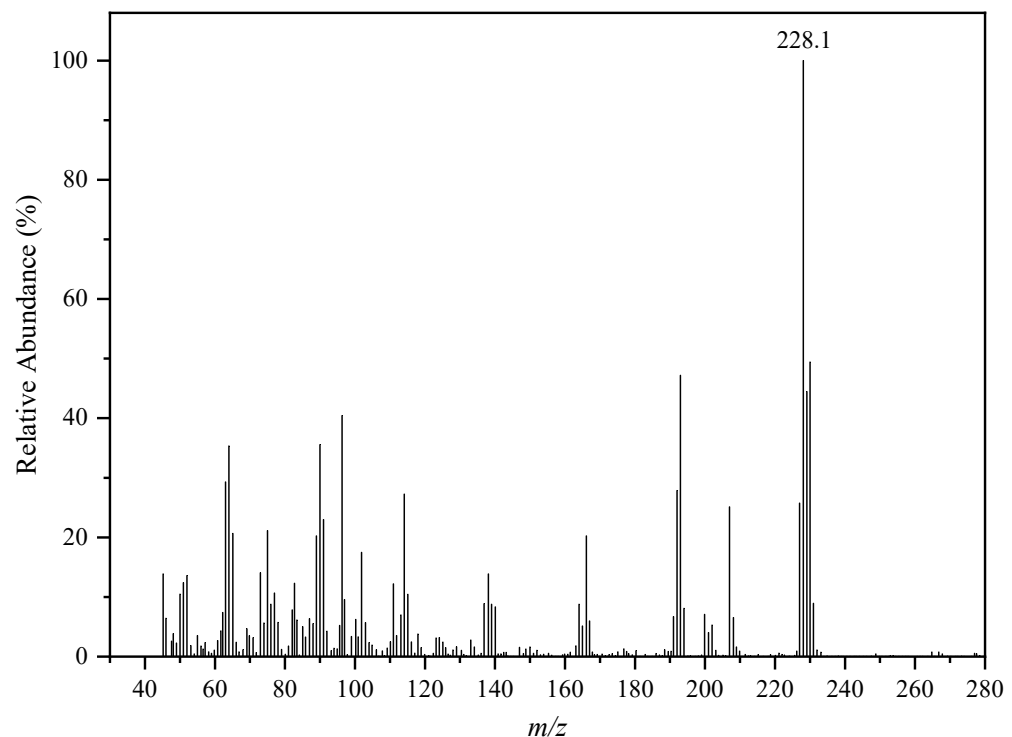
EI-MS: C₁₃H₉ClN₂, m/z (%) = 228.2 (100%) [M⁺].



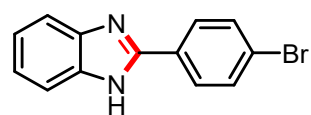
2-(2-chlorophenyl)-1*H*-benzo[*d*]imidazole (3h)



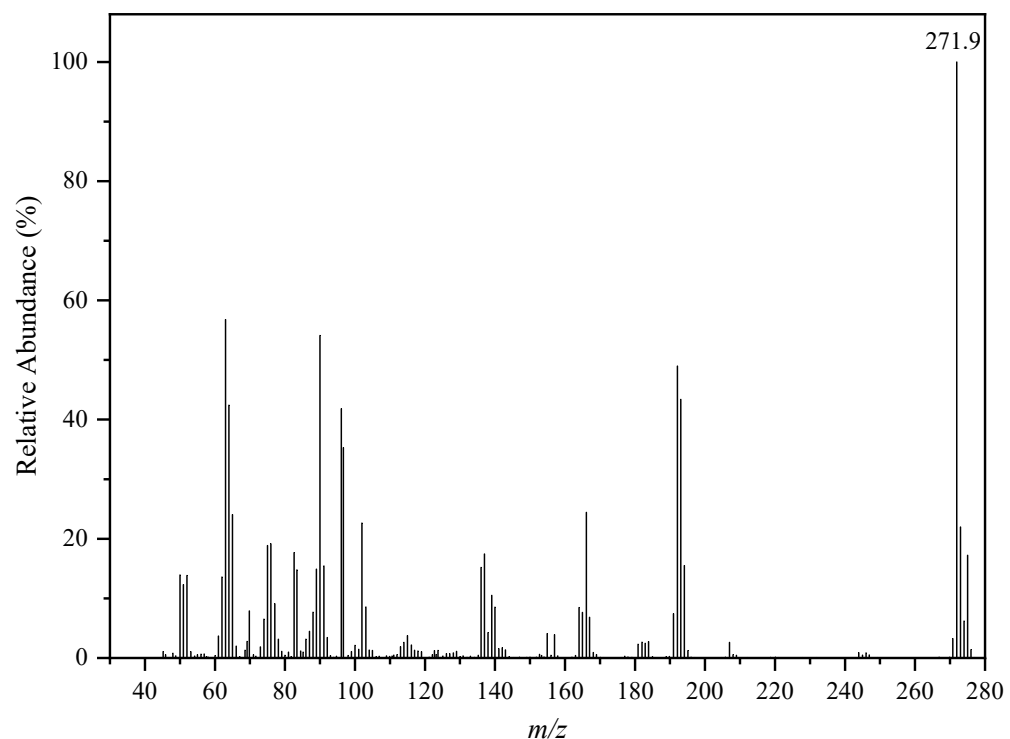
EI-MS: C₁₃H₉ClN₂, m/z (%) = 228.1 (100%) [M⁺].



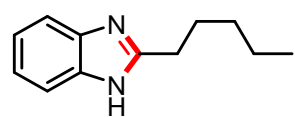
2-(4-bromophenyl)-1*H*-benzo[*d*]imidazole (3i)



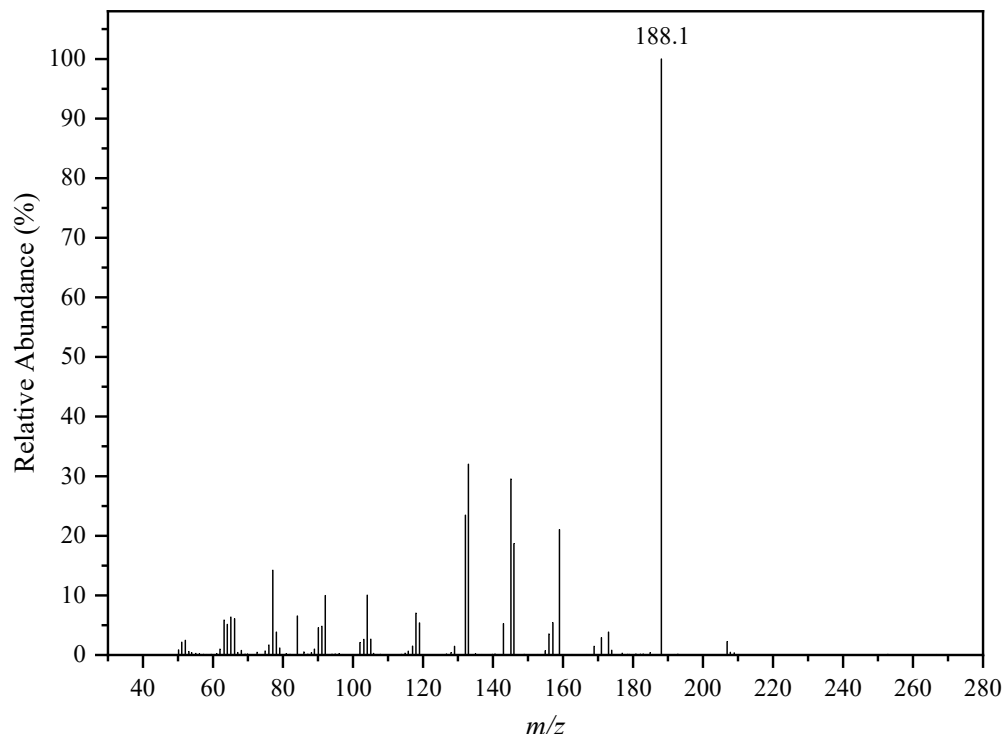
EI-MS: C₁₃H₉BrN₂, m/z (%) = 271.9 (100%) [M⁺].



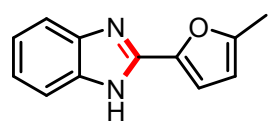
2-pentyl-1*H*-benzo[*d*]imidazole (3j)



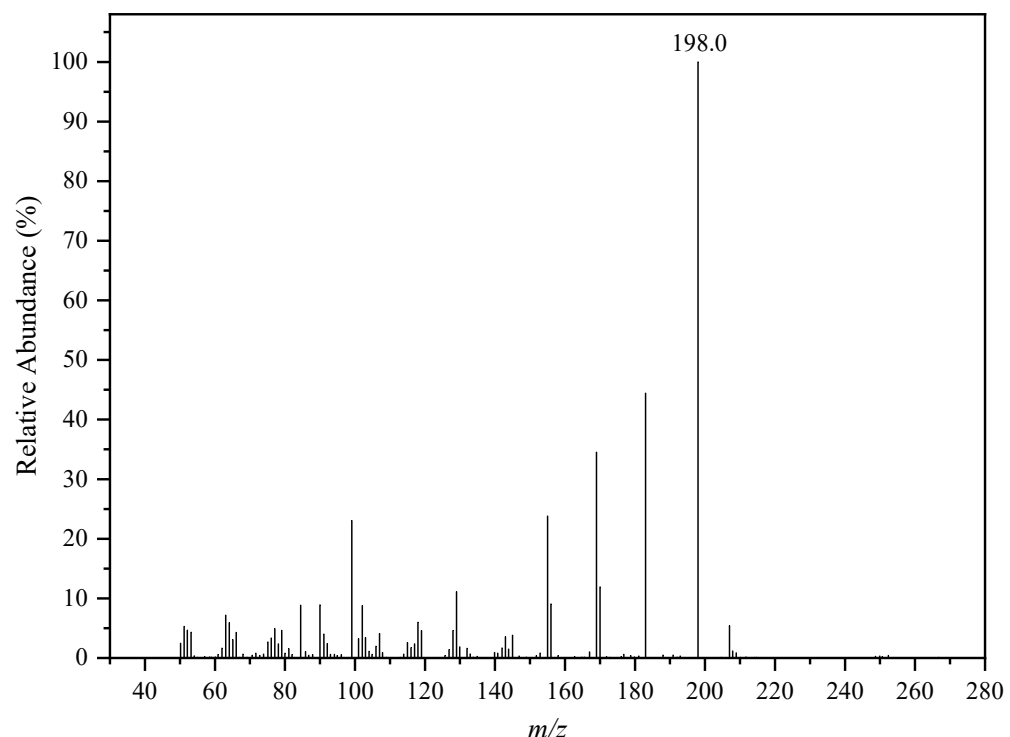
EI-MS: C₁₃H₉ClN₂, m/z (%) = 188.1 (100%) [M⁺].



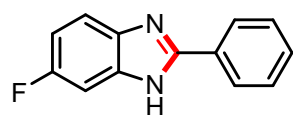
2-(5-methylfuran-2-yl)-1*H*-benzo[*d*]imidazole (3k)



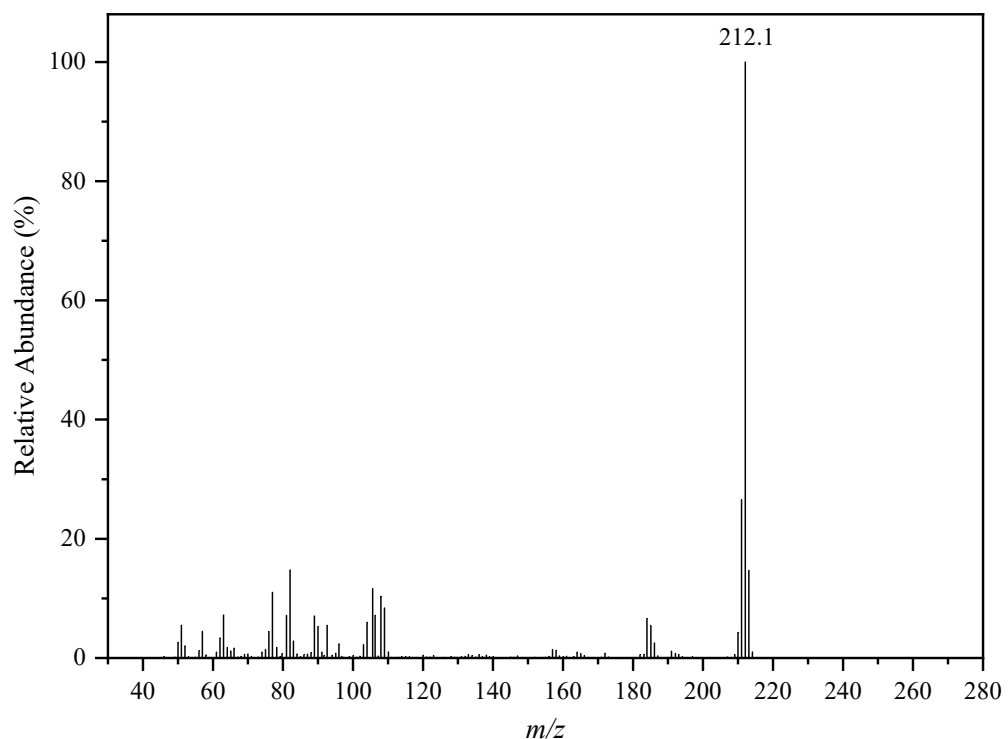
EI-MS: C₁₃H₉ClN₂, m/z (%) = 198.0 (100%) [M⁺].



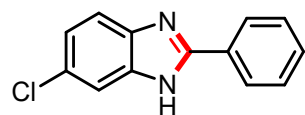
6-fluorine-2-phenyl-1*H*-benzo[*d*]imidazole (3l)



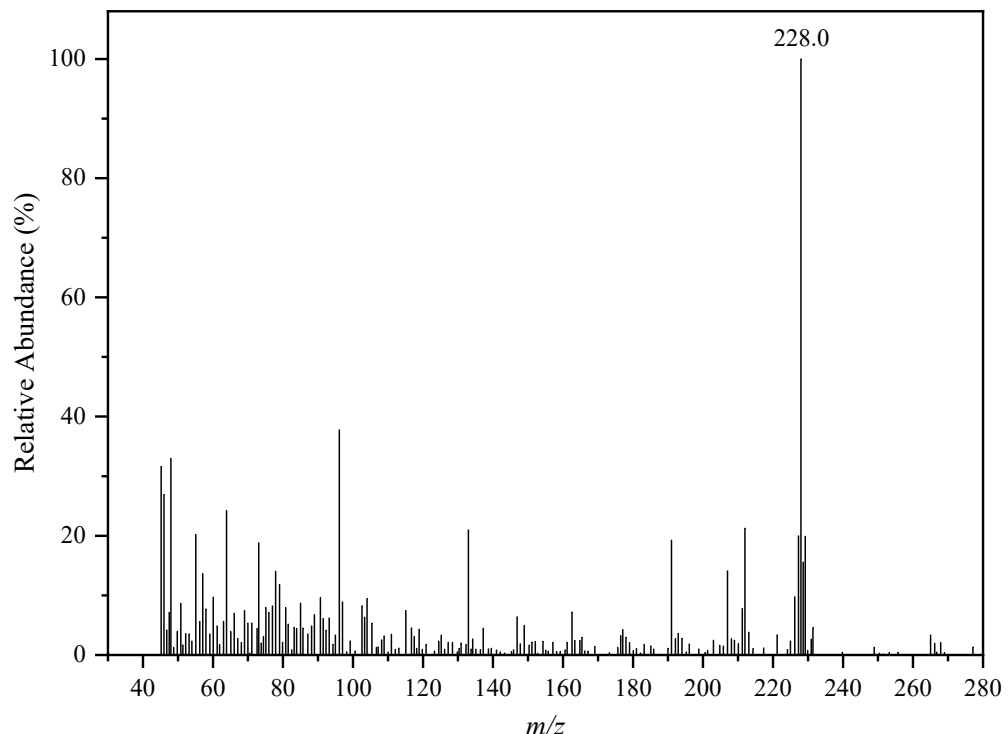
EI-MS: C₁₃H₉FN₂, m/z (%) = 212.1 (100%) [M⁺].



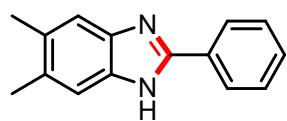
6-chloro-2-phenyl-1*H*-benzo[*d*]imidazole (3m)



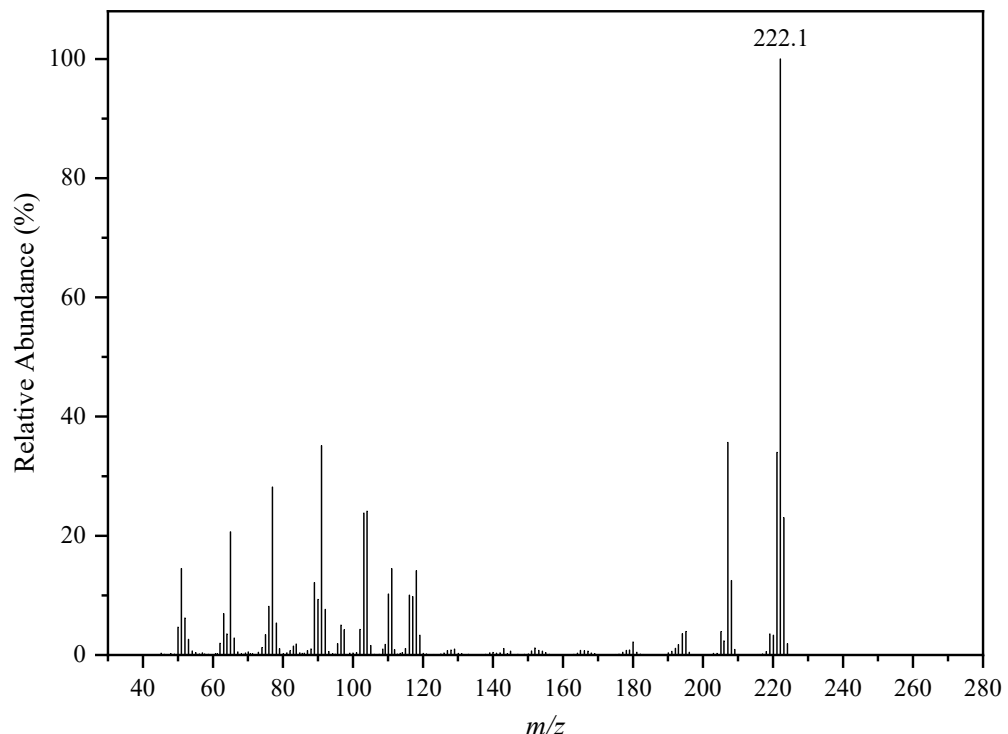
EI-MS: C₁₃H₉ClN₂, m/z (%) = 228.0 (100%) [M⁺].



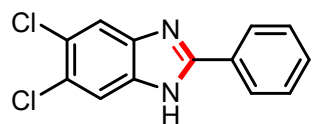
5,6-dimethyl-2-phenyl-1*H*-benzo[*d*]imidazole (3n)



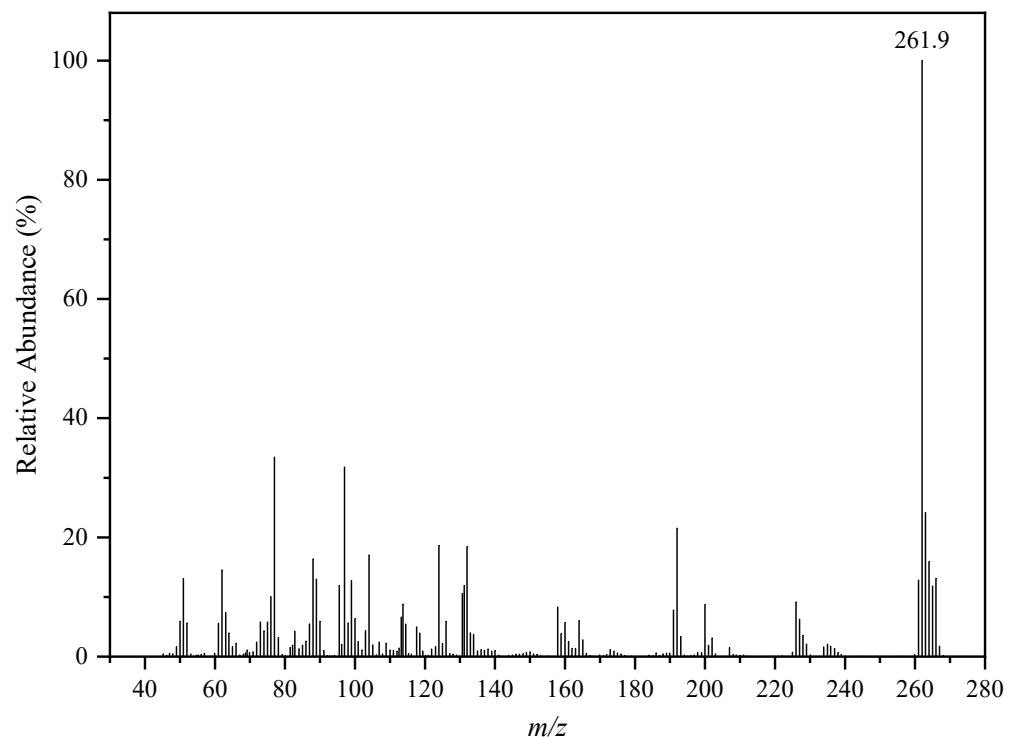
EI-MS: C₁₅H₁₄N₂, m/z (%) = 222.1 (100%) [M⁺].



5,6-dichloro-2-phenyl-1*H*-benzo[*d*]imidazole (3o)



EI-MS: C₁₃H₈Cl₂N₂, m/z (%) = 261.9 (100%) [M⁺].



5. Notes and References

- (1) Bruker, A. *APEX3 Package, APEX3, SAINT and SADABS*. **2016**.
- (2) (a) Spek, A. L. Single-Crystal Structure Validation with the Program *PLATON*. *J. Appl. Cryst.* **2003**, *36*, 7-13; (b) Spek, A. L. Structure Validation in Chemical Crystallography. *Acta Cryst.* **2009**, *D65*, 148-155; (c) Spek, A. L. What Makes a Crystal Structure Report Valid? *Inorg. Chim. Acta* **2018**, *470*, 232-237; (d) Dolomanov, O. V.; Bourhis, L. J.; Gildea, R. J.; Howard, J. A.; Puschmann, H. *OLEX2: A Complete Structure Solution, Refinement and Analysis Program*. *J. Appl. Cryst.* **2009**, *42*, 339-341; (e) Sheldrick, G. M. *SHELXT—Integrated Space-Group and Crystal-Structure Determination*. *Acta Cryst.* **2015**, *A71*, 3-8; (f) Sheldrick, G. M. Crystal Structure Refinement with *SHELXL*. *Acta Cryst.* **2015**, *C71*, 3-8.
- (3) (a) Brese, N.; O'keeffe, M. Bond-Valence Parameters for Solids. *Acta Cryst.* **1991**, *B47*, 192-197; (b) Brown, I.; Altermatt, D. Bond-Valence Parameters Obtained from a Systematic Analysis of the Inorganic Crystal Structure Database. *Acta Cryst.* **1985**, *B41*, 244-247.